TempTrend - Forecasting Global Warming Impacts

Roshan Muddaluru
College of Engineering & Applied Science
University of Colorado Boulder
Boulder, USA
roshan.muddaluru@colorado.edu

Satvik Ravikumar
College of Engineering & Applied Science
University of Colorado Boulder
Boulder, USA
satvik.ravikumar@colorado.edu

***Abstract*—Global temperature trends and their implications for climate change are investigated through comprehensive statistical analysis and machine learning approaches. Using historical temperature data from 1750 to the present, we analyze global, regional, and local temperature patterns across different countries, with a particular focus on Brazil, India, and the United States. It makes use of bootstrapping, hypothesis testing, and Bayesian analysis along with XGBoost and LightGBM-advanced machine learning models to forecast temperature. Temperature proves to be very different between regions; XGBoost tends to outperform others by R^2 = 0.93 when compared to LightGBM by R^2 = 0.91. From this, the tendency of a stable global upward trend was captured, especially during recent decades, and the effects it created differ among different parts of the Earth. This work provides valuable insights into the understanding of climate change patterns and supports the development of targeted mitigation strategies.**

***Index Terms*—global temperature, statistical analysis, regression, time-series**

I. Introduction

Global warming is one of the most significant challenges humanity faces today, with far-reaching implications for the environment, economies, and societies. The sustained increase in Earth's average temperature, driven by rising greenhouse gas concentrations, has triggered drastic changes in weather patterns, ecosystems, and resource availability. These shifts threaten biodiversity, disrupt human livelihoods, and create vulnerabilities in key economic sectors such as agriculture, infrastructure, and tourism. To address the wide-ranging impacts of global warming, it is essential to delve deeply into the historical and future trends of global temperatures, identify vulnerable regions, and propose strategies for mitigation and adaptation.

Examining global temperature trends over past centuries is fundamental to understanding the trajectory of climate change. By analyzing average, minimum, and maximum temperature changes over time, this study seeks to uncover patterns of accelerated warming in specific regions, identify seasonal variations, and detect anomalies that signal rapid climate shifts. Such insights are critical to determining the scale and scope of global warming and recognizing areas that are disproportionately affected.

This work is motivated by a series of pressing questions aimed at addressing the multifaceted impacts of climate change. What are the global average temperature trends over the past centuries, and how have these evolved across different regions, countries, or cities? Are certain regions disproportionately affected by rising temperatures, and if so, which ones show the highest temperature increases in recent decades? These questions help to identify vulnerable geographies and the extent of their exposure, which is essential for formulating region-specific strategies for adaptation.

The relationship between temperature changes and uncertainty variables also plays a vital role in understanding the nuances of climate modeling and prediction. Analyzing uncertainty over time sheds light on the reliability of temperature measurements and projections, enabling more informed decisions. Additionally, examining whether maximum and minimum temperatures have consistently increased over time provides a more detailed picture of the nature and intensity of warming trends.

The central research question this study addresses is "How can we forecast global and regional temperatures for the coming decades?" Using historical temperature trends, we forecast temperature changes over the next 10, 20, and 50 years. This question is critically important as accurate temperature forecasts enable policymakers and organizations to develop effective climate adaptation strategies and identify vulnerable regions and economic sectors before they face severe impacts. Our forward-looking analysis aims to identify regions with the steepest warming trajectories and the economic sectors that are most at risk, providing essential insights for long-term planning and resource allocation.

By integrating these elements, this work also seeks to map risks and opportunities linked to global warming. Vulnerable regions, such as coastal areas facing sea-level rise, will be highlighted, alongside sectors like agriculture that are highly sensitive to temperature variability. Furthermore, the study aims to assess the economic consequences of rising temperatures, such as increased cooling demands in urban areas, infrastructure stress, and agricultural losses, to guide infrastructure planning and resource allocation effectively.

In summary, this work addresses these pressing questions to provide actionable insights into the anticipation and mitigation of the economic and environmental impacts of global warming. By offering a comprehensive analysis of historical trends, regional disparities, and potential future scenarios, it aims to inform decision-makers, enabling them to implement robust

policies and strategies. This research ultimately aspires to support governments, industries, and communities in adapting to and mitigating the adverse effects of climate change, fostering resilience in the face of one of the most urgent challenges of our time.

The paper is arranged as follows: Section 2 analyzes the existing work in the study of global temperature trends from the past decades. A detailed discussion of the data is provided in Section 3. Section 4 demonstrates the intricate methodology details used throughout the work. Section 5 provides analysis and insights into the experimental results, and Section 6 reaches a conclusion, and offers some more potential directions for exploring the problem.

II. Related Work

In the era of big data meteorology, many scholars have done many studies on temperature prediction and have come up with rich theoretical results. For instance, [1] predicted the monthly average temperature of Australia and New Zealand using two machine learning algorithms. [2] came up with the latest ARIMA, Integrated Model, which can solve insufficient problems of data dependency and complexities in the prediction mechanism at present for current temperature data. It reduced the needed input of data and raised predictive accuracy. [3] suggested two temperature time series forecasting models, such as the linear combination non-parametric FDA regression model and the seasonal ARIMA, for improving accuracy. [4] proposed a new algorithm for outdoor temperature forecasting based on pattern approximation matching and, through experimental comparison, verified the effectiveness of the new algorithm. [5] applied artificial neural networks to forecast the Ararat Valley temperature in Armenia, in order to enhance the hourly air temperature forecast up to 24 h.

[6] proposed a framework based on LSTM deep learning networks for generating high spatial resolution hourly temperature predictions and demonstrated that LSTM networks outperform other traditional prediction techniques. [7] developed a seasonal ARIMA and LSTM based combination model for temperature prediction with high accuracy. [8] integrated the convolutional neural network and long short-term memory network into a new network (CNN-LSTM) and proved by experiments that the hourly temperature forecasted by CNN-LSTM model was highly consistent with the measured values. [9] proposed an improved deep ensemble machine learning framework based on machine learning and deep learning for the prediction of sensor-based indoor temperatures in urban environments in Australia. Experimental comparisons revealed that the DEML model showed high accuracy in different climate zones, seasons, and building types. [10] proposed the adaptive time-pattern network based on the deep time feature model, multi-time-pattern convolution module, and spatial attention mechanism module to predict temperature.

The gap that this work addresses is to provide a comprehensive comparative analysis between traditional time-series approaches and modern machine learning methods. This paper addresses this gap by conducting an thorough statistical analysis of global temperature trends over the past few decades on a few selected countries. This work compares the predictive capabilities of the time-series models with that of the regression models, providing valuable insights about forecasting the temperature and answering the research question.

III. Data Description

The dataset used in this study provides a record of the global average land and ocean temperature from 1750 into the present, thereby affording an invaluable asset by which to analyze the progression of climate trends through the ages. It includes information on the world average land temperatures in Celsius as well as the 95% confidence intervals for both averages and maximum land temperatures. It also highlights, with varied resolution, global trends, national-level variations, and subnational-level impacts on climate change. The country-specific temperature data reveals the national trend related to human activity, while the records sorted state-wise or regional level highlight subnational-level climate variation over population centers. Besides that, it also includes records with a particular focus on major metropolitan areas of the world to indicate localized climate change due to urbanization and year-round activities. The dataset, obtained from Berkeley Earth and curated on Kaggle, enables a granular review of global, regional, and local climate change for researchers interested in its wide implications.

A. Data Cleaning

Data cleaning was an important aspect that had to be done for this study to ensure reliability and accuracy of the analysis. There were a number of missing values in the dataset across multiple columns of temperatures, including averages and their uncertainties, as well as maximum and minimum temperature records. This was followed by the removal of rows containing missing values in these key columns. This ensured that the records analyzed within the dataset were complete and consistent. For dealing with the missing values, the method of interpolation was used after re-sampling the data to a monthly frequency.

In the city-level dataset of temperatures, there were about 175,426 rows with missing average temperatures and their uncertainty. Similarly, country and state level datasets had 32,651 and 25,648 records missing these two most important metrics, respectively. These records were excluded in order to maintain data integrity. The global missing values were also recorded in maximum, minimum, combined land and ocean temperatures, and their respective uncertainties at 1,200 missing records each. By filtering out the incomplete records, all datasets remained with zero missing values after cleaning and thus were strong enough for analysis. This cleaning process has allowed the dataset to give reliable insights into long-term temperature trends and their possible impacts, thus embedding the results of the study in consistent and high-quality data.

B. Exploratory Data Analysis

The first question this work answers is 'What are the global average temperature trends over the past centuries?' Fig. 1. shows a long-term view of global average temperature trends, illustrating how temperatures have changed over the past 250 years. The blue line represents the global average temperature, which shows an overall upward trend since the start of the Industrial Revolution, marked by the green vertical line. The red line indicates the 10-year moving average, highlighting the long-term warming pattern. The gray shading represents the uncertainty range, reflecting the natural variability in temperature measurements. The chart demonstrates that while there have been fluctuations, with both warm and cool periods, the global average temperature has been rising over the centuries, correlating with the onset of industrialization. This visualization gives a comprehensive perspective on the complex climate dynamics that have unfolded over the past two and a half centuries.

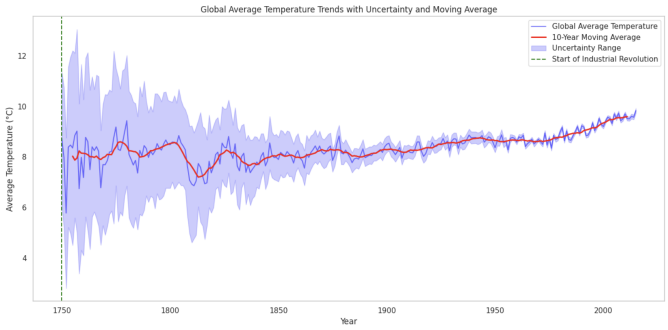

Fig. 1. Global average temperature trends.

Moving on to the next question to be answered, 'Is there a correlation between rising temperatures and specific regions (e.g., countries or cities)?' After computing the average annual temperature by country and filtering out a few countries for analysis, it is observed that there is significant variation in the temperature trends between the different countries. While they all generally exhibit an upward trajectory, the specific patterns and magnitudes of change differ notably. The United States, for instance, shows the most pronounced warming trend, with temperatures rising steadily over the past century. In contrast, China and India display more moderate warming trends, with some periods of temperature fluctuations. Brazil and Australia have relatively less pronounced temperature increases compared to the other countries shown.

Fig. 2. shows that the timing of major historical events, such as the Industrial Revolution in 1750 and the start of the Modern Era in 1900, are marked with vertical lines, suggesting that these pivotal moments may have influenced the observed temperature changes to some degree. The divergence in temperature trends between the countries also indicates that regional factors, in addition to global climate patterns, play an important role in shaping local temperature dynamics.

It can be noticed that Brazil stands out as having the strongest positive correlation at 0.85. This suggests that in

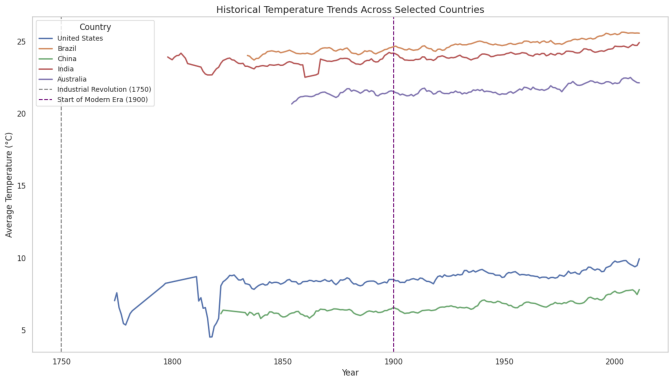

Fig. 2. Historical temperature across countries of interest

Brazil, as the years have progressed, temperatures have tended to increase in a fairly linear fashion. China also exhibits a relatively high positive correlation of 0.74, indicating a moderately strong link between time and increasing temperatures. India, Australia, and the United States show weaker, but still positive, correlations of 0.59, 0.66, and 0.49 respectively. This implies that while temperatures have trended upwards over time in these countries, the relationship is not as strongly linear as in Brazil and China.

Now, to answer the question, 'What is the relationship between temperature and uncertainty variables over time?', we plot the Fig. 3. that shows presents a compelling visualization of the relationship between global average temperature and temperature uncertainty over time, revealing several important insights. Firstly, the blue line depicting the global average temperature shows significant fluctuations, with both warming and cooling periods, but an overall upward trend is evident, indicating that temperatures have been rising steadily since 1850. Meanwhile, the red line representing temperature uncertainty demonstrates a noteworthy decrease over the same period, from a high of around 0.8°C in the late 19th century to a low of 0.2°C in the present day. This suggests that our ability to accurately measure and understand global temperatures has improved considerably. Interestingly, an inverse relationship

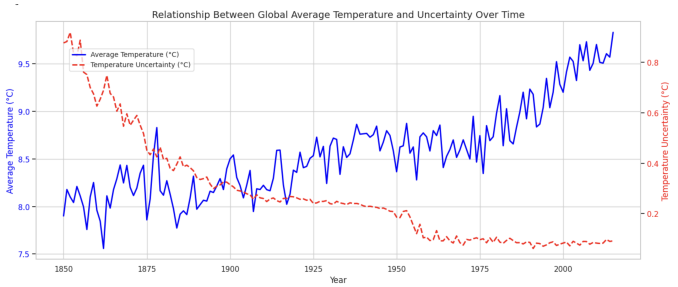

Fig. 3. Relationship between Global average temperature and uncertainty over time

appears to exist between the global average temperature and temperature uncertainty. When temperatures are higher, the uncertainty tends to be lower, and vice versa, implying that

more stable climatic conditions are associated with greater measurement precision. The data also exhibits pronounced short-term variations, underscoring the complex and dynamic nature of global climate patterns, which are influenced by a myriad of natural and human-induced factors. Despite these short-term fluctuations, the overarching long-term trend points to a gradual increase in global average temperature, accompanied by a decrease in temperature uncertainty. This observation highlights the growing robustness of our understanding of climate change, even as challenges and uncertainties remain. Z-score normalization as shown in eq. (1). was done on the data as it is essential for the models to rely on the scale of the input features and as we all know it has a mean of 0 and a standard deviation of 1.

$$z = \frac{x - \mu}{\sigma} \tag{1}$$

The heatmap Fig. 4. shows the correlations between different temperature-related variables, ranging in value from -1 to 1. High positive correlations exist between land average temperature and land max temperature (1.00), and between land and ocean average temperature (1.00); these variables move together. On the other hand, strong negative correlation exists between land average temperature uncertainty and land and ocean average temperature uncertainty (-0.84), meaning one goes up when the other goes down. For weaker correlations, such as those from temperature difference to land minimum temperature uncertainty, lighter colors will be used. In sum, this heat map promotes knowledge about the relationship in temperature variables of both land and ocean and helps analyze climatic patterns.

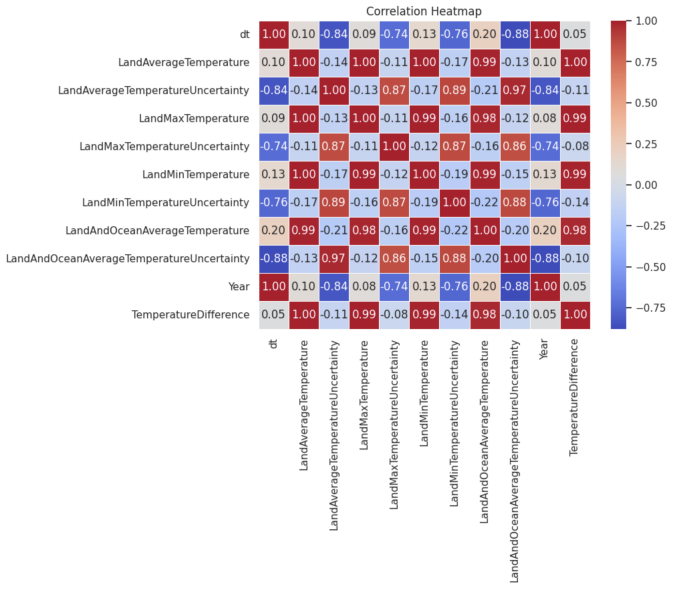

Fig. 4. Correlation heatmap matrix

EDA was done on 3 specific countries: Brazil, United States and India. Graphs of average temperature over time are shown for Brazil (1840–2020), India (1800–2000), and the United States (1800–2000). Each graph reveals smoothed data represented by a different color: green for Brazil, red for India, and blue for the United States. These graphs show a general view of the changes in temperatures over long periods and climatic variability in these regions.

We find that all three regions indeed express main temperature fluctuations over their periods: it has considerable peaks and valleys, hence indicating much variability and changes. There are three distinctive patterns, but an upward trend can be seen across all three graphs, signaling general warming over time. Indeed, this is consistent with the global pattern of climate change, especially the observed increase in average temperatures during the 20th century.

Certain periods within the graphs pinpoint periods of rapid temperature rise that could be associated with specific environmental or anthropogenic factors that have altered regional climates. However, the nature of such changes is not similar across regions, including the following:

- Brazil: A gradual trend indicates warming with observable variability, indicating long-term alterations in the climate of the region as shown in Fig. 5.
- India: Temperature changes look more capricious; large swings without any specific consistent warming pattern over the total period as seen in Fig. 6.
- United States: Fig. 7. shows that the data reflects a combination of substantial variability and warming, though the temperature changes in the United States also display an erratic pattern similar to India.

These long-term temperature trends put into perspective the need for continued climate monitoring and data collection to understand regional climate dynamics and responses to environmental and human-induced factors. This will be important in analyzing regional climate variability, identifying trends, and addressing the challenges posed by climate change. A

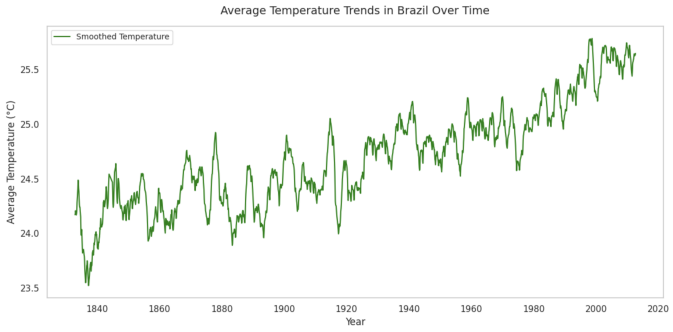

Fig. 5. Average temperature trend in Brazil

statistical technique called the Dickey-Fuller test is used to assess if a time series is stationary. When a series is said to be stationary, its statistical characteristics—such as its mean, variance, and autocorrelation—remain consistent throughout time. In time series analysis, where many modeling techniques require the data to remain steady, the test is very pertinent. The ADF Statistic computed a test statistic -2.5017. This is checked against critical values at various confidence levels,

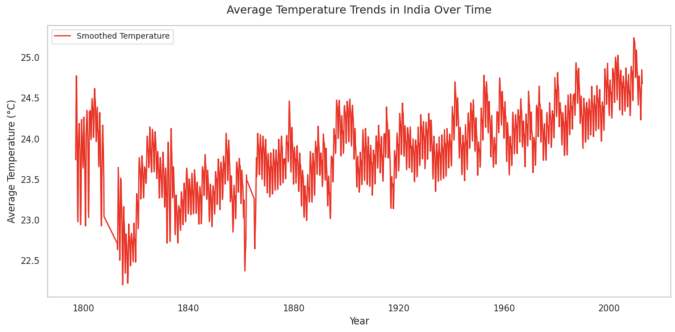

Fig. 6. Average temperature trend in India

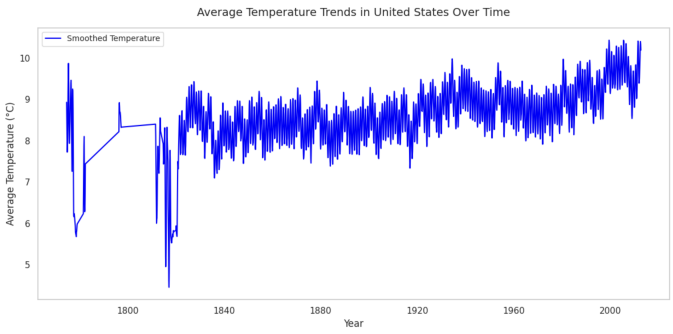

Fig. 7. Average temperature trend in United States

namely 1%, 5%, and 10%, in order to conclude whether the series is stationary or not. The computed p-value is 0.1150 which exceeds the generally accepted 0.05 level and, therefore, fails to provide sufficient evidence to reject the null hypothesis. The corresponding critical values at 1%, 5%, and 10% are -3.43, -2.86, and -2.57, respectively. The ADF statistic is less than these critical values, which again supports the null hypothesis. It appears that the time series is non-stationary. Therefore, it may possess a unit root, and consequently, the series would show trends, seasonality, or other forms of non-stationarity. Very often, to proceed with time series modeling, one has to make the series stationary, which might be done by differencing, de-trending, or applying transformations, such as logarithmic or seasonal decomposition. A non-stationary series can result in untrustworthy model estimates and predictions. This will, in return, enhance the accuracy and reliability of any subsequent analyses or forecasting models.

Fig. 8. shows global temperatures with 95% confidence intervals from 1750 to 2000, showing the variability and uncertainty in the data. Confidence intervals as shown in eq. (2). quantify the range within which the true values are likely to lie, with wider intervals in earlier periods reflecting sparse data and narrower intervals in recent decades indicating improved data accuracy.

$$\text{CI} = \hat{\mu} \pm z \cdot \frac{\sigma}{\sqrt{n}} \tag{2}$$

Global temperatures have seen large variations over the past 250 years, with periods of warming and cooling. The general trend is one of rising temperatures, with the late 20th century considerably warmer than earlier periods. There are also short-term increases and decreases in temperature, probably due to such factors as volcanic eruptions, solar variability, and other climate forcing. The latest points reflect a continuing trend of rising global temperatures and significant warming of the modern era. This graph puts the historical temperature changes into perspective, highlighting both natural variability and the accelerated warming of recent decades.

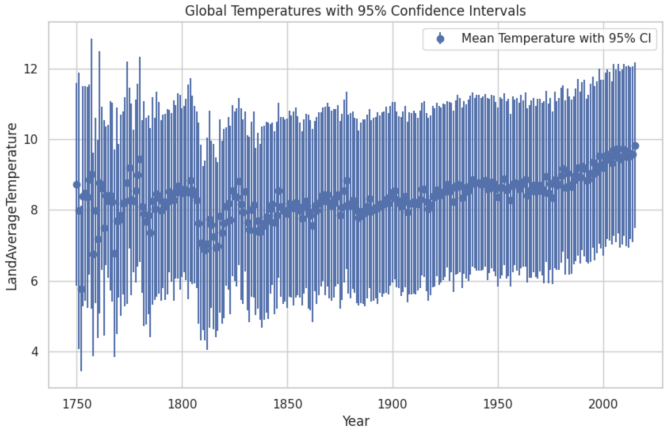

Fig. 8. Global temperature with 95% CI

Bootstrapping (eq. (3).) is a resampling technique that works by estimating the distribution of a statistic, usually repeated sampling from the observed data with replacement. It is used to assess the uncertainty of the estimated mean temperature. Fig. 9. shows a bootstrap distribution of mean temperatures centered around 8.5 degrees and represents the estimated global average. The bell-shaped curve suggests a normal distribution with a temperature range from approximately 8.2 to 8.6 degrees, indicating large variability.

$$\hat{\theta}^* = \frac{1}{B} \sum_{b=1}^{B} \theta_b^* \tag{3}$$

The 95% confidence interval, given by the lower and upper bound lines, extends from 8.23 to 8.52 degrees and shows the uncertainty for the mean. The distribution has a left-skewed shape; hence, the probability of recording cooler temperatures is higher than that of recording warmer ones. This plot shows the uncertainty and confidence of the estimated global mean temperature, reflecting the robustness of climate data and projections. It clearly shows the central tendency and range of variability. According to the CLT, all these distributions of the sample means approach a normal distribution with increased sample size irrespective of the distribution of the original data. It forms the very basis for applying the methods for a normal distribution in various problems arising. The plot shows a bell curve which indicates that the distribution is a normal distribution.

Hypothesis testing is a statistical methodology that deals with drawing inferences or conclusions about a population

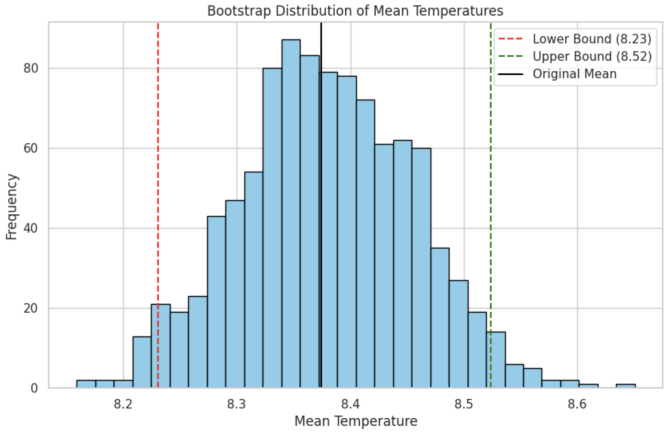

Fig. 9. Bootstrap distribution of mean global temperature

based on sample data. It helps determine whether there is sufficient evidence to support a particular claim or hypothesis. The process involves the formulation of a null hypothesis (which assumes no effect or difference) and an alternative hypothesis, followed by the use of a test statistic to assess the evidence provided by the sample data. This analysis was designed to test if the average temperature was significantly different from a hypothesized value of 15.0° C. The result of the hypothesis test shows that the t-statistic is -85.27 and the p-value is 0.0000, far below the 0.05 significance level. Based on this, we reject the null hypothesis, concluding that the average temperature differs significantly from 15.0° C. This indicates that the mean temperature recorded in the data is far from the hypothesized value of 15.0°C and hence, there is a very strong evidence to suggest that the mean is different.

Point estimates are the single value statistics used to estimate parameters. They summarize some aspects of the dataset like measures of central tendency, spread, and variability and describe characteristics about the data. The mean temperature is 8.37°C, representing the average temperature across the dataset. The median temperature is a little higher at 8.61°C, showing the middle value in the data, hence a slight skew toward lower temperatures. The variance of 19.20 reflects the degree to which individual temperatures differ from the mean, and there is a rather high spread in the data. This variability is further quantified by a standard deviation of 4.38°C, which means there is usually a deviation from the mean by this temperature. The recorded minimum is -2.08°C, while the recorded maximum is 19.02°C. It follows that there was a wide variation in the values. Lastly, 1.32% of the temperatures are above 15.0°C.

Bayes' theorem as shown in eq. (4). is a very fundamental concept in probability theory, describing the probability of a certain event given prior knowledge of conditions that relate to the occurrence of the event. It forms a wide basis for statistical inferences and decision-making, including the updating of our beliefs toward an event based on new evidence. The theorem in this context, therefore, helps in deducing the probability of high temperatures based on recent years, using the information from both high temperature occurrences and the recent timeframe.

$$P(A|B) = \frac{P(B|A) \cdot P(A)}{P(B)} \tag{4}$$

From the calculated probabilities, the chances of a high temperature (above 15°) happening within the dataset are quite minimal, standing at just 1%. The probability of its occurrence within the recent years, 2000 to 2020, stands at 6%. The conditional probability that high temperatures have occurred in recent years, given that the temperature was high, is 31%. However, this does not mean that the probability of high temperatures given recent years is also 31%, which in fact is only 7%, because even though high temperatures are more likely in recent years, the general occurrence of high temperatures remains rare.

IV. Methodology

The study would analyze and predict the average temperature over an extended period for countries such as Brazil, India, and the United States using time series and regression models. Time series will use the forecasting technique through ARIMA, auto-ARIMA, and SARIMA, while on the other hand, using XGBoost and LightGBM allows a very flexible and robust regression.

The AutoRegressive Integrated Moving Average (ARIMA) whose formula shown in eq. (5). is a statistical model for time series analysis and prediction. It combines three features: the autoregressive component, or the one responsible for dependencies on past values; the integrated component, responsible for stationarity through differencing; and the moving average, which accounts for dependencies of present forecast errors. Here, y_t is the value at time t_i, ϕ_i are the autoregressive coefficients, θ_i are the moving average coefficients, and ϵ_t is the error term at time t.

$$y_t = \phi_1 y_{t-1} + \cdots + \phi_p y_{t-p} + \theta_1 \epsilon_{t-1} + \cdots + \theta_q \epsilon_{t-q} + \epsilon_t \tag{5}$$

ARIMA is especially useful in analyzing temperature trends by identifying and modeling the underlying pattern to ensure that long-term forecasting is done accurately.

SARIMA, or Seasonal ARIMA, extends the ARIMA model by including seasonal autoregressive, differencing, and moving average components as seen in eq. (6). These additions make it ideal for datasets with periodic patterns, thus enabling it to capture seasonal variations in temperature trends.

$$\Phi(B^s) y_t = \Theta(B^s) \epsilon_t \tag{6}$$

where $\Phi(B^s)y_t$ and $\Theta(B^s)$ are the seasonal autoregressive and moving average polynomials respectively, and s is the seasonal period. Auto-ARIMA automates the process of selecting optimal ARIMA parameters, reducing manual tuning and ensuring the best-fit model for the data.

For regression analysis, XGBoost and LightGBM will be implemented. XGBoost (Extreme Gradient Boosting) a shown

in eq. (7). is an ensemble learning method that uses decision trees and gradient boosting to optimize predictions.

$$\text{Obj} = \sum_{i=1}^{n} l(y_i, \hat{y}_i) + \sum_{k=1}^{K} \Omega(f_k) \tag{7}$$

Here, $l(y_i, \hat{y}_i)$ is the loss function, $\Omega(f_k)$ is the regularization term, and (f_k) represents the base learners. XGBoost excels in capturing complex interactions in data, making it suitable for predicting temperature variations influenced by multiple factors.

LightGBM is another gradient boosting framework that is designed for high performance with large datasets. It is based on leaf-wise tree growth with the aim of achieving both optimal accuracy and efficiency. The loss function remains almost similar to XGBoost, but due to the unique tree-growing algorithm in this algorithm, it enables faster training and good scalability. These models provide a comprehensive framework for analyzing temperature trends. Time series models will uncover temporal dependencies and periodic behaviors, while regression models will integrate additional explanatory variables to improve predictive accuracy. Together, these methods offer robust insights into regional temperature changes over extended periods.

XGBoost Regression also includes several parameters to optimize its performance and prevent overfitting. Its objective function minimizes squared error, hence accurately predicting the values by minimizing the difference between actual and predicted values. The usage of 1000 boosting iterations will make the model iteratively refine the predictions. A learning rate of 0.1 is chosen for gradual optimization to converge stably. A maximum tree depth of 6 controls the complexity of individual trees, preventing overfitting by limiting their ability to overfit specific patterns. Subsampling ratios of 0.8 for rows and columns introduce randomness that improves generalization by reducing dependence on particular features or data points. Regularization is applied with L_1 and L_2 penalties ($\alpha = 0.01$ and $\lambda = 1$, respectively) to control model complexity and impose sparsity, enhancing robustness. Besides that, a minimum child weight of 1 ensures statistically significant splits, further reducing overfitting.

The LightGBM regression model follows a similar process, with parameters optimized for efficiency and accuracy. The objective function minimizes regression error to predict continuous outcomes effectively. Performance is iteratively enhanced in 1000 iterations. The learning rate is set at 0.1 to provide stable optimization. A maximum depth of 10 allows for capturing complex patterns without leading to overfitting. Sub-sampling ratios are set to 0.8 for both rows and columns to give diversity in splits, thereby improving generalization. Regularization terms include: L_1 and L_2 penalties ($\alpha = 0.01$ and $\lambda = 1$), respectively, handle the model complexity and sparsity in feature weights. Minimum child weight of 1 for statistically valid splits makes the model more reliable with less sacrifice in predictive power.

The performance metrics employed in this study to evaluate the models include Root Mean Squared Error (RMSE), Mean Absolute Error (MAE), Mean Squared Error (MSE), and R^2 as shown in eq. (8-11). These metrics provide a comprehensive understanding of the model's predictive accuracy and reliability. The RMSE is the standard deviation of residuals that describes the degree of deviation between predicted and actual values. The lower the value, the better the model. On the contrary, MAE computes the average magnitude of the absolute prediction errors.

$$\text{RMSE} = \sqrt{\frac{1}{n}\sum_{i=1}^{n}(y_i - \hat{y}_i)^2} \tag{8}$$

$$\text{MAE} = \frac{1}{n}\sum_{i=1}^{n}|y_i - \hat{y}_i| \tag{9}$$

$$\text{MSE} = \frac{1}{n}\sum_{i=1}^{n}(y_i - \hat{y}_i)^2 \tag{10}$$

$$R^2 = 1 - \frac{\sum_{i=1}^{n}(y_i - \hat{y}_i)^2}{\sum_{i=1}^{n}(y_i - \bar{y})^2} \tag{11}$$

It gives an unequivocal measure of accuracy in its own right, without considering the direction of error. Because MSE is quadratic, larger errors are emphasized much more than smaller ones, which makes it susceptible to outliers. R^2, finally, gives the percentage of variance in the dependent variable that is predictable from the independent variable, with a high value indicating that the model is very predictive of the actual outcomes.

V. Results and Analysis

To address the central research question of forecasting global and regional temperatures for coming decades, we evaluated three sophisticated modeling approaches: XGBoost, LightGBM, and SARIMA. The comparative analysis of these models provides robust insights into their capabilities for long-term temperature forecasting, which is crucial for climate adaptation planning. In comparing the models' forecasting capabilities, we examined key performance metrics including RMSE, MAE, MSE, and R^2 as shown in Table 1. These metrics are particularly relevant for assessing the models' ability to provide accurate long-term temperature predictions that policymakers can rely on.

XGBoost demonstrated superior forecasting potential with an RMSE of 1.17, MAE of 0.83, MSE of 1.38, and an R^2 value of 0.93, suggesting it could provide more reliable long-term temperature projections. LightGBM showed slightly lower but still robust forecasting capabilities with an RMSE of 1.27, MAE of 0.89, MSE of 1.61, and an R^2 value of 0.916. The strong performance of both models, particularly XGBoost's higher R^2 value, indicates their suitability for generating the decadal temperature forecasts needed for climate adaptation strategies.

To ensure the robustness of our forecasting approach, we further validated these results against a SARIMA(3,0,3) model. The SARIMA model showed strong statistical significance across all parameters (p-values less than 0.001) and achieved an AIC of 9700.38, demonstrating its capability to capture temporal patterns in temperature variations. The model's sigma2 value of 1.16 aligns well with the prediction variance seen in XGBoost (1.17) and LightGBM (1.27), providing additional confidence in our forecasting framework. While the Ljung-Box test statistic (Q=3.03, p=0.08) confirmed no significant autocorrelation in the residuals, the Jarque-Bera test revealed non-normal distribution of residuals (p less than 0.001) with slight negative skewness (-0.44) and high kurtosis (13.03). Despite the SARIMA model's strong statistical foundation, the machine learning approaches, especially XGBoost, demonstrated superior predictive capabilities, likely due to their ability to capture complex, non-linear patterns in temperature trends – a crucial advantage for long-term temperature forecasting across different regions and timeframes.

TABLE I
PERFORMANCE OF MODELS

Models	**Performance Metrics**			
	RMSE	**MAE**	**MSE**	**R-squared**
XGBoost	1.17	0.83	1.38	0.93
LightGBM	1.27	0.89	1.61	0.91

The scatter plot for XGBoost shows a strong linear relationship between actual and predicted values, as most points are closely aligned with the diagonal line, representing perfect predictions. This indicates that XGBoost consistently captures the underlying patterns in the data with high accuracy. The scatter plot of LightGBM in Fig. 10. also shows a high degree of correlation between actual and predicted values, but with a bit more deviation from the diagonal line than in XGBoost. These visual observations are further supported by the numerical metrics, as XGBoost had lower error rates and higher explained variance. Both models seem to work well for the prediction of coffee import values, with XGBoost performing marginally better. The higher value of R^2 for XGBoost indicates that it explains a greater proportion of variance in the data and is thus more reliable to carry out the task.

LightGBM, though a little less accurate, is still promising because of its computational efficiency and the capability to handle large datasets. Results further underline that tree-based ensemble models are suitable for this regression problem, providing robust yet interpretable predictions that are aligned with actual values.

VI. CONCLUSION AND FUTURE SCOPE

The trends in global temperature will provide an understanding of its relation to global warming, considering that advanced regression models predict a rise in temperatures. From these models, XGBoost and LightGBM are found to be the top two best models that have accurately captured

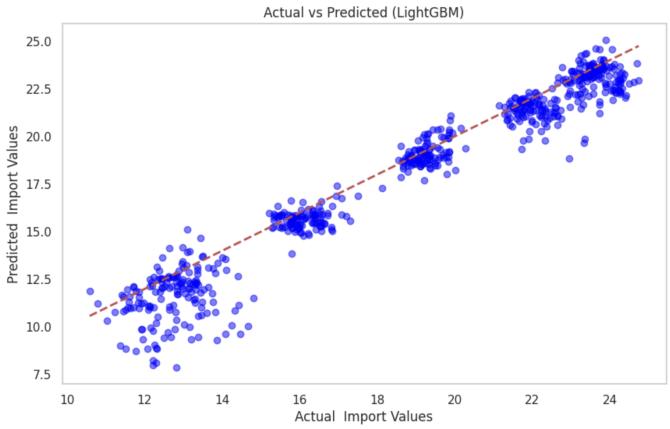

Fig. 10. Actual vs predicted for LightGBM

temperature changes reflected by key metrics such as RMSE and R^2. These results point out an increase in global temperatures significantly, which directly relates to extreme weather conditions, meltdown of ice caps, rising sea levels-all causes behind climate change. The need is evident for data-driven strategies in regards to mitigating these changes by promoting sustainability on a global scale.

Other statistical methods besides predictive modeling were used in an attempt to ensure robustness of analysis. Assumptions about statistical significance had been approved through hypothesis testing, model variability by bootstrapping, normality assumptions using CLT-justifying findings that could be obtained from more robust results. Bayes' Theorem revised probability estimates with new data, while point estimates, confidence intervals, and z-score normalization were helpful in the evaluation of model accuracy and scaling of data effectively. These statistical approaches were the backbone in this study for deeper insights into the connection of global temperature changes with global warming.

The work carried out here could further be refined in the future using more detailed regional and seasonal temperature records for a fine-grained view of the climate dynamics. Furthermore, investigation into the potential use of such models in determining the socio-economic consequences of global warming, with particular emphasis on agriculture, biodiversity, and public health, would also be highly valued. Advanced AI techniques integrated into climate modeling may improve its prediction accuracy and provide much better tools for policymakers in the implementation of effective solutions. In fact, considering the worsening climate crisis, such research and global collaboration on the protection of the future of our planet are more urgently needed than ever.

ACKNOWLEDGMENT

We would like to take this opportunity to express our gratitude to University of Colorado Boulder and all our professors for their continuous support, which enabled us to carry out this research. Their encouragement and guidance have been invaluable throughout the completion of this work.

REFERENCES

[1] Azevedo, Vitor G., and Lucila MS Campos. "Combination of forecasts for the price of crude oil on the spot market." *International Journal of Production Research* 54, no. 17 (2016): 5219-5235.

[2] Wang, Huan, Jiejun Huang, Han Zhou, Lixue Zhao, and Yanbin Yuan. "An integrated variational mode decomposition and ARIMA model to forecast air temperature." *Sustainability* 11, no. 15 (2019): 4018.

[3] Curceac, Stelian, Camille Ternynck, Taha BMJ Ouarda, Fateh Chebana, and Sophie Dabo Niang. "Short-term air temperature forecasting using Nonparametric Functional Data Analysis and SARMA models." *Environmental Modelling & Software* 111 (2019): 394-408.

[4] Wang, Yuying, Yan Bai, Liu Yang, and Honglian Li. "Short time air temperature prediction using pattern approximate matching." *Energy and Buildings* 244 (2021): 111036.

[5] Astsatryan, Hrachya, Hayk Grigoryan, Aghasi Poghosyan, Rita Abrahamyan, Shushanik Asmaryan, Vahagn Muradyan, Garegin Tepanosyan, Yaniss Guigoz, and Gregory Giuliani. "Air temperature forecasting using artificial neural network for Ararat valley." *Earth Science Informatics* 14 (2021): 711-722.

[6] Yu, Manzhu, Fangcao Xu, Weiming Hu, Jian Sun, and Guido Cervone. "Using Long Short-Term Memory (LSTM) and Internet of Things (IoT) for localized surface temperature forecasting in an urban environment." *IEEE Access* 9 (2021): 137406-137418

[7] Li, Guoqiang, and Ning Yang. "A Hybrid SARIMA-LSTM Model for Air Temperature Forecasting." *Advanced Theory and Simulations* 6, no. 2 (2023): 2200502.

[8] Hou, Jingwei, Yanjuan Wang, Ji Zhou, and Qiong Tian. "Prediction of hourly air temperature based on CNN–LSTM." *Geomatics, Natural Hazards and Risk* 13, no. 1 (2022): 1962-1986.

[9] Yu, Wenhua, Bahareh Nakisa, Emran Ali, Seng W. Loke, Svetlana Stevanovic, and Yuming Guo. "Sensor-based indoor air temperature prediction using deep ensemble machine learning: An Australian urban environment case study." *Urban Climate* 51 (2023): 101599.

[10] Yang, Jinqi, Yu Guo, Tao Chen, Lang Qiao, and Yang Wang. "Data-driven prediction of greenhouse aquaponics air temperature based on adaptive time pattern network." *Environmental Science and Pollution Research* 30, no. 16 (2023): 48546-48558.